Vibro driving testing in confined space for offshore wind farm application

An Ninh Ta [i)], Olivier Jean [ii)]

i) Engineer, PhD, Geotechnical Department, Saipem, 1 Av San Fernando, Montigny le Bretonneux, France.

ii) Engineer, Head of Geotechnical Department, Saipem, 1 Av San Fernando, Montigny le Bretonneux, France.

ABSTRACT

An onshore vibro driving testing of large-scale piles (2.5 m diameter) was carried out in order to validate an innovative foundation design that is needed to overcome challenging soil conditions encountered at an offshore wind farm in France. The foundation concept named DSD (drill-sand-drive) is to replace the hard soils using drilling by engineered granulars that are then compacted to design density though which monopiles are vibrodriven. Three tests were conducted covering different levels of soil compaction from low to very high and that was closely controlled using CPT. The pile driving monitoring comprised PDA sensors, vibro hammer parameters, crane hook load as well as water pressure along the external pile shaft to evaluate the liquefaction extent. The tests ultimately produced the confinement configuration induced by the drilled hole and the surrounding stiff soils and provide evidence of its impact on noticeable amplification of vibro compaction and vibro driving.

Keywords: vibro driving, offshore wind, confined space, vibro compaction, monopile, granular materials

1 INTRODUCTION

In the framework of an offshore wind farm development in France, monopile foundations of 7.0 to 8.0 m diameter have to be installed in difficult soils consisting of alternate weak to medium strong limestone and stiff to very hard clay with interbedded cemented layers. While direct impact driving into these soils presents too high risks, bored piles of XXL monopile under large cyclic loading suffers strong records, especially the guarantee of subsea grouting quality between the monopiles and the drilled holes.

In this context, a novel foundation concept named DSD (drill-sand-drive) was made and is composed of following steps: (1) drilling down to the target, (2) filling with selected granular materials, (3) vibro compaction to the design density and (4) vibro driving the monopile. Each step represents one separate operation and can be conducted by different vessels.

In order to ascertain the feasibility of the concept and further refine the design, a physical large scale testing campaign was carried out onshore (OPT: onshore pile test). Testing setup, obtained results, associated interpretation and conclusions are presented in this paper.

2 SCALED ONSHORE TESTING SETUP

The test setup schema is presented in Fig. 1. All the steps of the DSD concept were followed. It is important to highlight that the monopile foundations will be vibro driven in a confined medium, both in terms of lateral pressure and water pressure dissipation. Indeed, the external in-place soils (either limestone rock or hard clay) are both considered as impervious (very low permeability) and they provide rather high lateral stiffness. This critical aspect is simulated by a closed steel casing built within a rock formation.

A large-scale test (R=1/3, the ratio between the pile test diameter and the offshore monopile diameter) was adopted. Large scale test was preferred to enable the observation and monitoring of the mechanisms: water pressure build up, granular density change, pile coring behavior etc. during vibro driving tests.

The scaling application was conducted to reproduce the same mechanisms and behaviors as expected in real full-scale conditions. The ratio was applied on governing parameters comprising the size of the casing, the annular thickness, the pile test geometries, the penetration length, the vibro hammer weight and the vibro hammer power (see Table 1).

The OPT pile tip shape is identical to the monopile's: with a bevel toward inside the pile (Fig. 2). This aims to direct more filling materials inside and

limit the increase of density of sand at the annulus part easing the vibro driving.

Three vibro driving tests were conducted into increasing soil density: non-compacted filling materials (OPT-1), well compacted filling materials (OPT-3) and maximum compacted filling materials (OPT-2). Cone penetration tests (CPT) were done before and after vibro driving, before and after vibro compaction to monitor density changes.

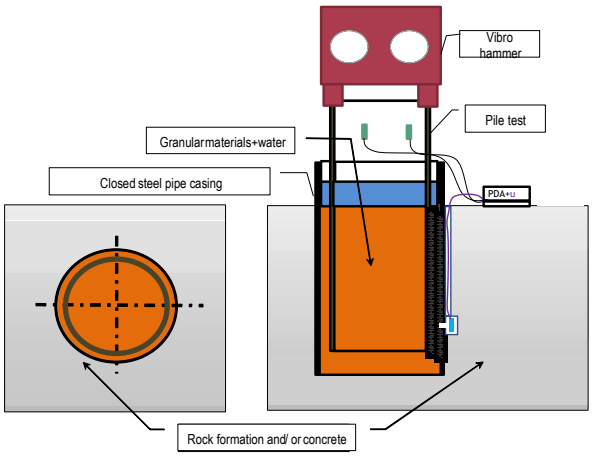

Fig. 1. Vibro pile driving tests schema.

Table 1. Scale application.

Item	Unit	Scale
Pile test OD	m	R
Pile test thickness	m	R
Pile test embedment	m	R
Pile test weight	ton	R3
Casing OD	m	R
Annulus thickness between pile test and casing	m	R
Added steel volume / granular material volume	%	1
Vibro hammer weight	ton	R^2
Vibro hammer eccentric moment	kg.m	R^2

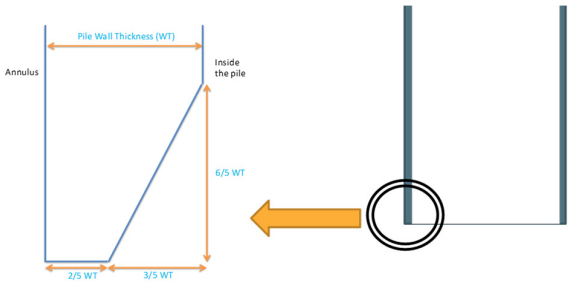

Fig. 2. Pile tip shape.

During vibro driving, monitoring was performed using (1) a pile driving analyzer (PDA) equipment to measure the transferred energy from the vibro hammer to the pile, the stresses in the pile and (2) pore water pressure gauges all along the internal casing surface to record water pressure build up / dissipation process in the annulus between the pile and the casing.

Besides, vibro compaction parameters, vibro hammer driving parameters, hook load of the crane were all recorded too. This allowed gathering the inputs necessary to back analyze the vibro pile driving process and the behavior of piles driven inside a confined space.

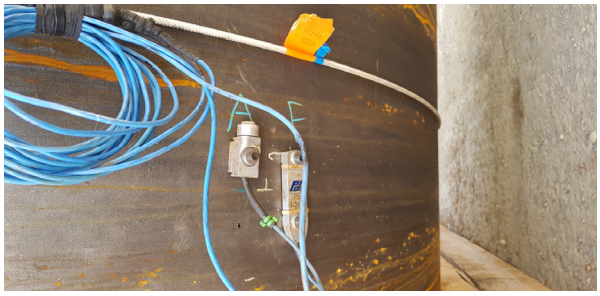

Fig. 3. PDA equipment.

Fig. 3. OPT tests with 250 M PTC vibro – End of vibro drive.

3 TEST RESULTS

The onshore pile tests (OPT) produced quite a large volume of valuable data, and relevant results related to vibro driving in confined space are presented hereafter.

Vibro compaction parameters of OPT-2 and OPT-3 (no compaction for OPT-1) are presented in Fig. 4 and Fig. 5 respectively. While the oil pressure was set at the same range (180 to 280 bar), more compaction steps were used at OPT-2 (every 0.5 m step instead of every 1.0 m step at OPT-3).

Vibro driving parameters of OPT-1, 2 and 3 are presented in Fig. 6, Fig. 7 and Fig. 8 respectively. At start of drive, one or two driving stops were needed to verify the pile verticality and positioning to avoid clash with the casing. At end of drive, one stop was needed to ensure no clash between the casing head and the PDA sensors. No vibro drive stop was due to soil resistance as the penetration speed was rather fast. Indeed, for all OPT tests, it took less than five (5) minutes of effective

vibro drive.

As anticipated in vibro driving prediction analysis, the measured stresses using PDA sensors were rather low, limited to 20 MPa (for example, see OPT-1 record in Fig. 9). The difference of measures from several sensors around the pile could be explained by the fact that the sensors were close to the pile head and one sensor may be closer to the vibro hammer gripper.

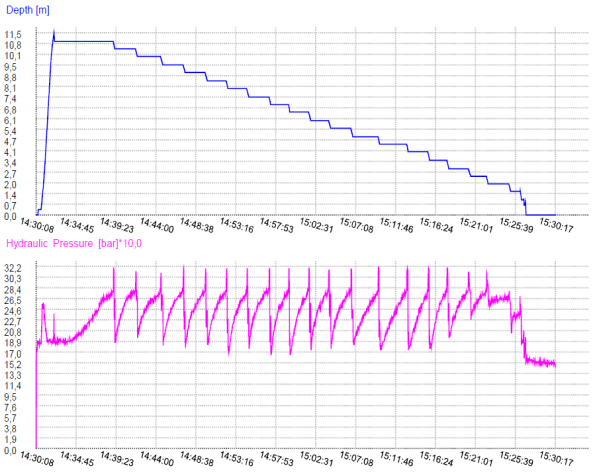

Fig. 4 OPT-2 Vibro compaction record.

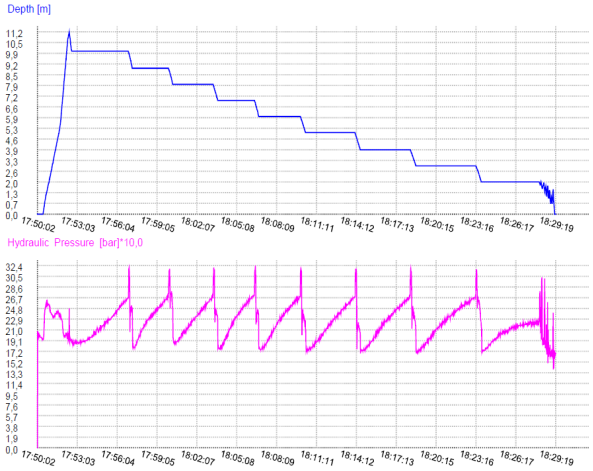

Fig. 5. OPT-3 Vibro compaction record.

Water pressure records (every 2 meters along one internal side of the casing) were quite similar for all OPT tests and the results of OPT-2 are selected for presentation in Fig. 10. Measured water pressures equal to theoretical hydrostatic pressures from the start of drive till about 1 m of pile penetration. From 3.5 m of pile penetration, total water pressure reaches the total vertical pressure at the top 5 m depth and it progressively reduces to the hydrostatic one at about 8, 9 m depth. Dissipation was fast since the water pressure was back to the hydrostatic one just few minutes after the end of vibro drive.

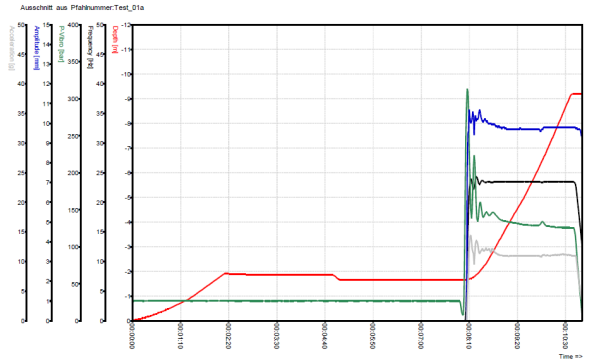

Fig. 6. OPT-1 Vibro driving record.

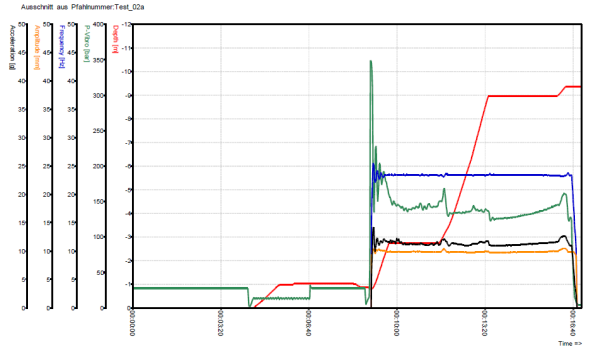

Fig. 7. OPT-2 Vibro driving record.

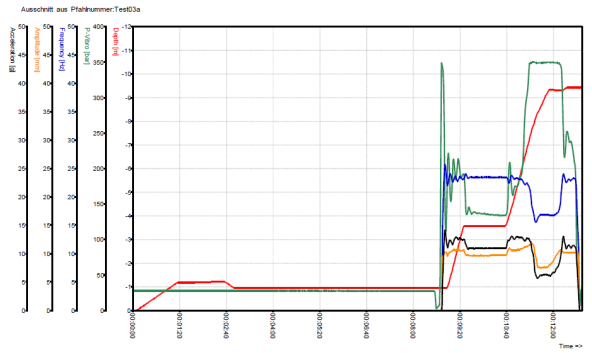

Fig. 8. OPT-3 Vibro driving record.

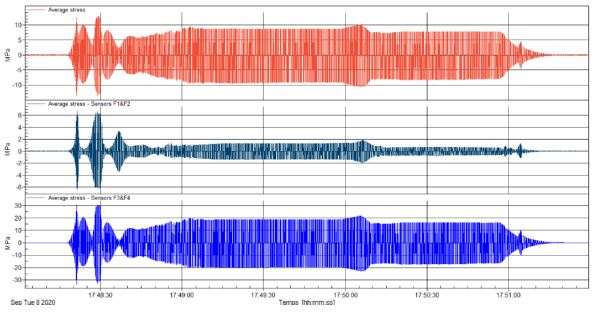

Fig. 9. OPT-1 PDA stress on steel pile record.

CPT tests were performed after the vibro compaction for the OPT-2 and OPT-3 to evaluate the

vibro compaction efficiency. CPT tests were as well carried out after the vibro driving for all the three OPT to assess possible impact of vibro driving on the compacity of the granular material.

The CPT results are presented together in Fig. 11. Since the CPT truck was set on the casing tip of about 1 m above the soil surface and to prevent the CPT rods from bending, backfill was added on topsoil surface while conducting CPT. This corresponds to negative depth values in Fig. 11. All CPT were run to target except for two CPT 3 hours after vibro compaction at OPT-2 and OPT-3 (refusals at about 6 m depth). High values of cone tip resistance q_c (> 20 MPa, even between 40 – 50 MPa) and sleeve friction f_s (> 100 kPa) were observed at OPT-2 and OPT-3 after vibro compaction while rather low values are noted for OPT-1. Vibro driving more or less modified CPT results of OPT-1 and OPT-3 while reduction of q_c and f_s at OPT-2 is noticeable.

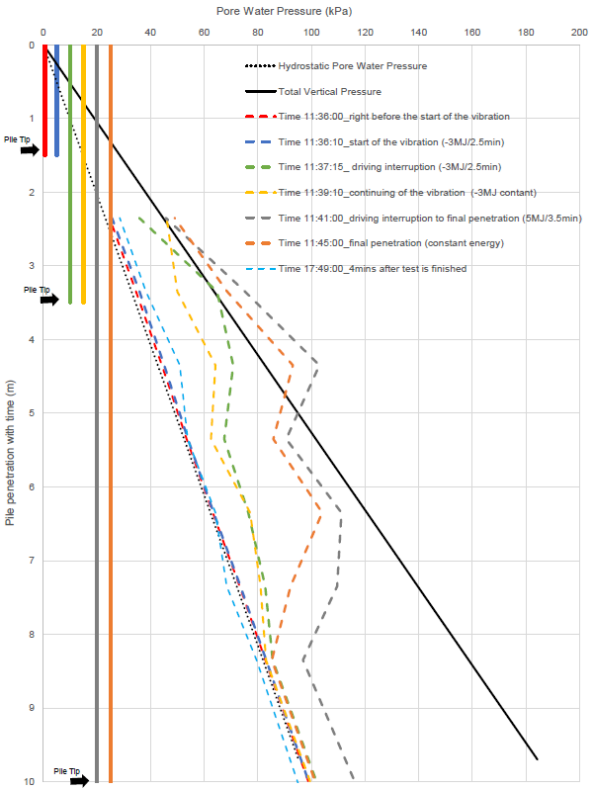

Fig. 10. OPT-2 Water pressure record.

4 INTERPRETATION AND DISCUSSIONS

4.1 Vibro compaction efficiency and density management of granular material

Since all the ideas behind the DSD concept is to replace challenging existing soils by an engineered material whose characteristics can be designed and managed, the control of the relative density, a key parameter of filling granulars, is of prime importance and is therefore further analyzed and discussed. The filling granular relative density was computed for all OPT as follows.

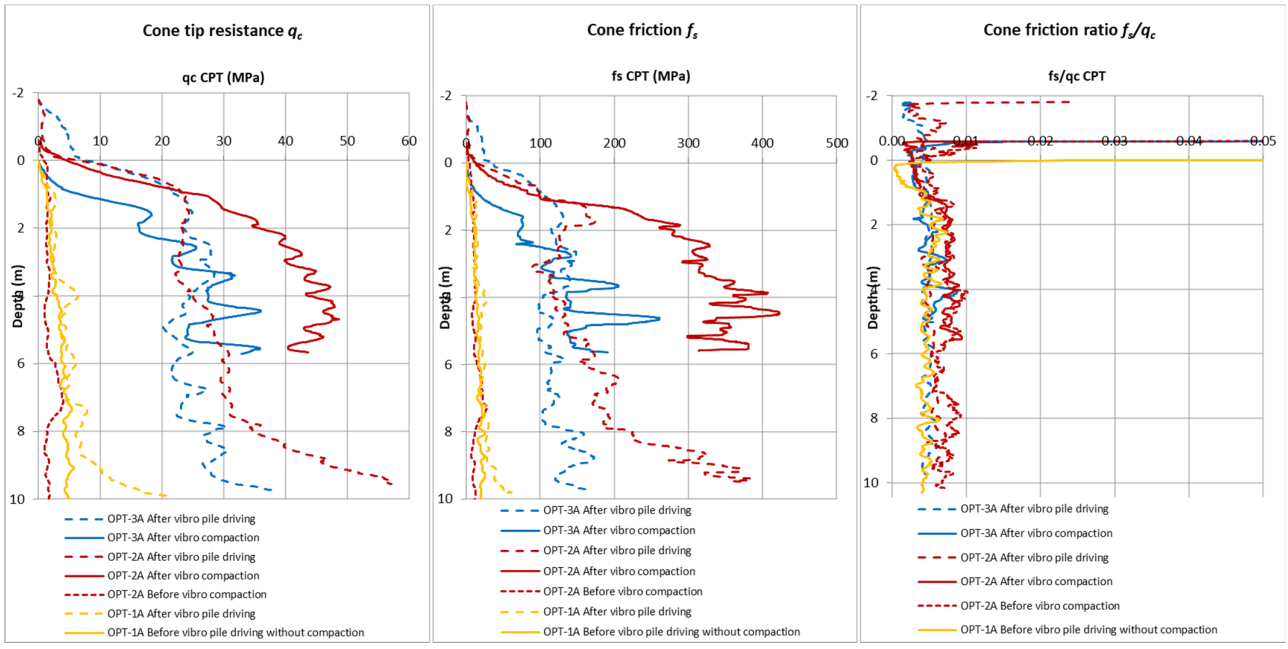

Fig. 11 CPT results of all OPT 1, 2 and 3.

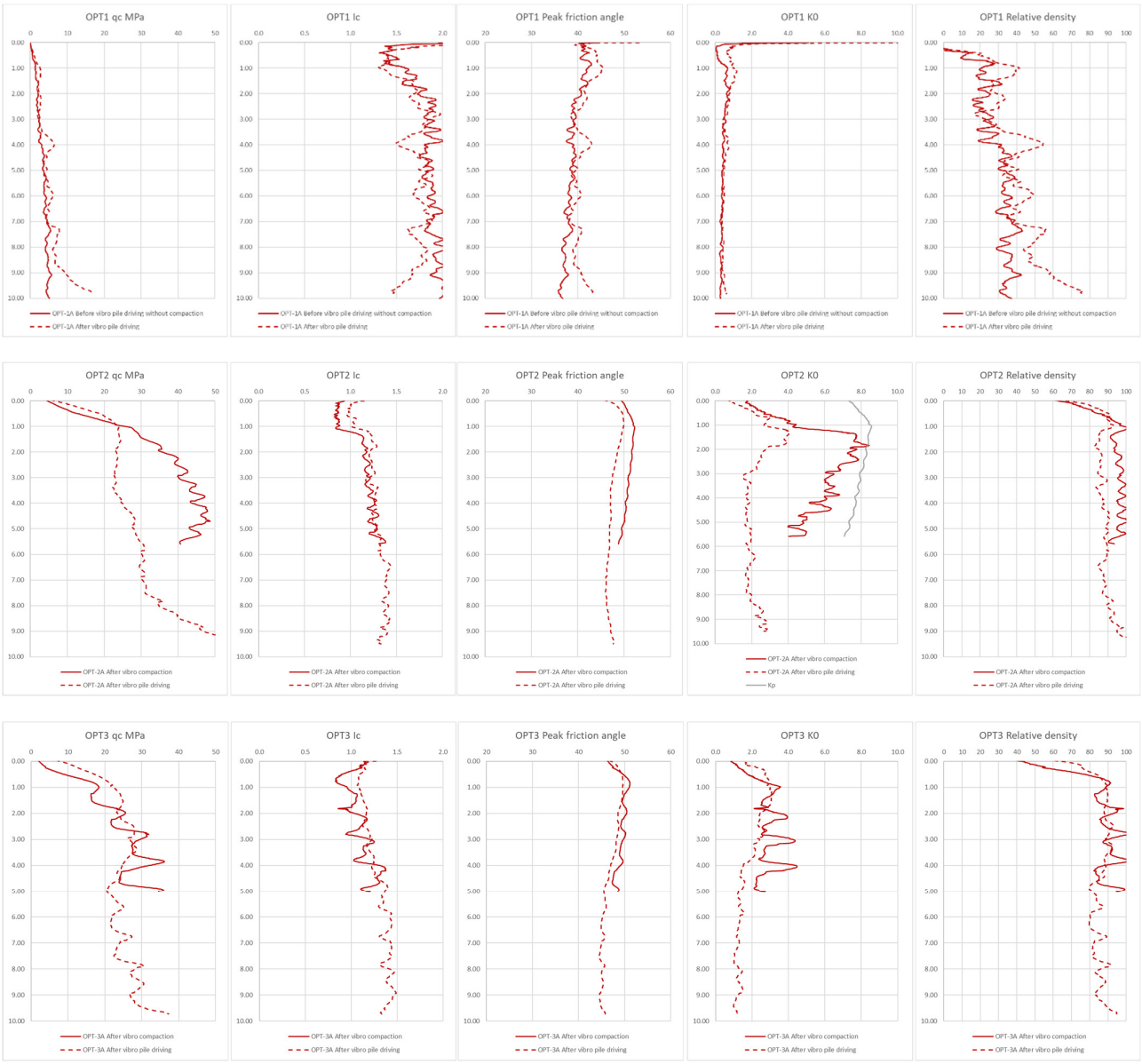

Fig. 12 CPT interpretation and relative density determination.

Using (Robertson et Cabal, 2015), soil behavior type index I_c and peak friction angle ϕ, are computed:

$$I_c = ((3.47 - logQ_t)^2 + (logF_r + 1.22)^2)^{0.5} \quad (1)$$

Where:

Q_t = normalized cone penetration resistance (dimensionless) = $(q_t - \sigma_{v0})/\sigma'_{v0}$

F_r = normalized friction ratio, in % $=(f_s/(q_t - \sigma_{v0})) \times 100\%$

$$tan\phi' = \frac{1}{2.68}\left[log\left(\frac{q_c}{\sigma'_{v0}}\right) + 0.29\right] \quad (2)$$

Subsequently, the coefficient of lateral earth pressure K_0 (ratio of the effective horizontal to vertical *in situ* soil stresses) is estimated as suggested by (Massarsch, 2002) as follows:

$$f_s = K_0 \sigma'_{v0} \tan(\phi') \quad (3)$$

Finally, the relative density is computed as per (Jamiolkowski et al, 2003):

$$D_r = \frac{1}{2.96} ln\left[\frac{{q_c(z)}/{p_a}}{24.94\left(\frac{\sigma' m(z)}{p_a}\right)^{0.46}}\right] \quad (4)$$

Where:

$\sigma' m(z)$ is the effective mean stress at depth z,

$\sigma' m(z) = (1/3)(\sigma' v0(z) + 2\sigma' h(z))$

$\sigma' h(z)$ is the effective horizontal stress at depth z, computed from the vertical one and K_0 ratio.

p_a is the atmospheric pressure (100 kPa).

Using the same paper, the obtained relative density

was corrected for saturated as it was OPT tests (and at offshore conditions). Detailed results of sand relative density computation are presented in Fig. 12.

Soil behavior type index I_c results, all below 2.0, are well in line with the selected filling material nature: a clean sand. Though the same sand was used for all tests, the I_c can slightly vary and is depending on compacity level (higher the density, lower the I_c).

As can be seen from the relative density determination equation (n°4), the density value depends both on the cone tip resistance and the confining pressure. Therefore, K_0 ratio needs to be properly estimated and ideally measured. In this paper, it is computed through the measured sleeve friction. The K_0 of non-compacted sand at OPT-1 is about 0.4 – 0.5 and is well expected for normally consolidated sands. On the other hand, the K_0 of OPT-2 and OPT-3 after vibro compaction are significantly higher (above 2.0), especially at the OPT-2 where K_0 can reach 6.0 and 8.0 at some depths, approaching the passive earth pressure (K_p). Increase of horizontal pressure at vibro compaction was reported in the literature, see (Massarsch, 2002), though this level of amplification was thought to result from the confinement configuration of the tests. Equally, the confinement allowed excellent levels of compaction at OPT-2 (around 95%) and OPT-3 (around 90%), above the usual values in free field condition.

The vibro driving modified the density of the filling material. At OPT-1, the relative density slightly increased from 25-35% (top-bottom part respectively) to 30-45%. At OPT-3, the average relative density did not seem to change (remains around 90% for the compared part with available data at top 5-6 m depth). The 1 m step used at vibro compaction that is visible at relative density curve was somehow smoothen with the vibro driving. At OPT-2, the relative density slightly reduced from around 95% to 85-90% (for the compared part). The vibro driving could have released some extra horizontal stress caused during the vibro compaction as demonstrated by clear reduction of K_0 after vibro driving. For both OPT-2 and OPT-3, the final relative densities are well above the value needed for the monopile foundation design.

4.2 Vibro driving and liquefaction

For all granular densities, from loose (OPT-1) to dense and very dense (OPT-3 and OPT-2), the vibro driving was fast and easy. The penetration rate was entirely directed by the crane lowering speed.

A less easy vibro driving had been predicted. Indeed, the available space is limited, by a rather stiff drilled hole in true scale and by a closed steel casing in OPT, the insertion of the steel pile volume could further increase the density of the sand and make the vibro driving more difficult into very dense sand. This easy vibro driving could possibly be explained by an amplification of the liquefaction of the granular material during vibro driving as there is only limited upward dissipation path (compared to radial dissipation in free field condition). This liquefaction phenomenon was corroborated thanks to the measurement of water pressure along the annulus space demonstrating the fully liquefied sand at the top five meters and over excess pressure of few meters below this depth.

As well, during pile removal using vibro hammer, little extraction force was needed. Probably, the liquefied sand in a close medium helped increase the buoyancy of the steel pile.

The special pile tip shape with inside bevel was believed to contribute to direct more sands inside the pile. Nevertheless, it is not possible to confirm this through the available topsoil level monitoring.

4.3 Offshore full-scale anticipation

The scale OPT tests are designed to reproduce the same mechanisms at full scale offshore. The vibro compaction is expected to be efficient and the vibro driving feasibility is ensured. Regarding the vibro compaction, due the large size offshore (around 9 m diameter compared to 2.5 m at OPT), several compaction points are planned with anticipated optimization thanks to the confined configuration. Field trial tests will help to confirm and validate the final compaction design. The vibro driving could cause and take advantage of rather large depths of liquefaction of filling materials. The liquefaction depth could be up to 3 times the one observed at OPT.

5 CONCLUSIONS

This paper presents a novel installation concept and its validation through large scale onshore pile tests.

The observation of confinement effect was the key to explain significant amplification of the efficiency of both the vibro compaction and the vibro driving. Very high compacity of filling granular materials can be expected but does not undermine the feasibility of vibro driving.

It is believed that valuable information is shared in this paper as contribution to bring innovative and economic foundation solutions for offshore wind.

REFERENCES

1) Massarsch, K. R., 2002. Effects of Vibratory Compaction. TransVib 2002 – *International Conference on Vibratory Pile Driving and Deep Soil Compaction*. Louvain-la-Neuve. Keynote Lecture, pp. 33 – 42.

2) Jamiolkowski, M., Lo Presti, D. C. F. And Manassero, M. (2003), Evaluation of Relative Density and Shear Strength of Sands from CPT and DMT, in Germaine, J. T., Sheahan, T. C. and Whitman, R. V. (Eds.)

3) Robertson P. K. and Cabal (Robertson) K. L. (2015): Guide to cone penetration testing for geotechnical engineering.